# $O_2$-generating $MnO_2$ nanoparticles for enhanced photodynamic therapy of bladder cancer by ameliorating hypoxia

Tingsheng Lin,[a,†] Xiaozhi Zhao,[a,†] Sheng Zhao,[b] Hang Yu[a], Wenmin Cao[a], Wei Chen[a], Hui Wei,[b,*] and Hongqian Guo[a,*]

[a]Department of Urology, Drum Tower Hospital, Medical School of Nanjing University, Institute of Urology, Nanjing University, Nanjing, Jiangsu 210008, China.

[b]Department of Biomedical Engineering, College of Engineering and Applied Sciences, Collaborative Innovation Center of Chemistry for Life Sciences, Nanjing National Laboratory of Microstructures, Nanjing University, Nanjing, Jiangsu 210093, China.

**Email:** dr.ghq@nju.edu.cn; **Tel:** +86-136-0517-1690

**Email:** weihui@nju.edu.cn; **Tel:** +86-25-83593272; **Fax:** +86-25-83594648; **Web:** weilab.nju.edu.cn

**Table of contents**

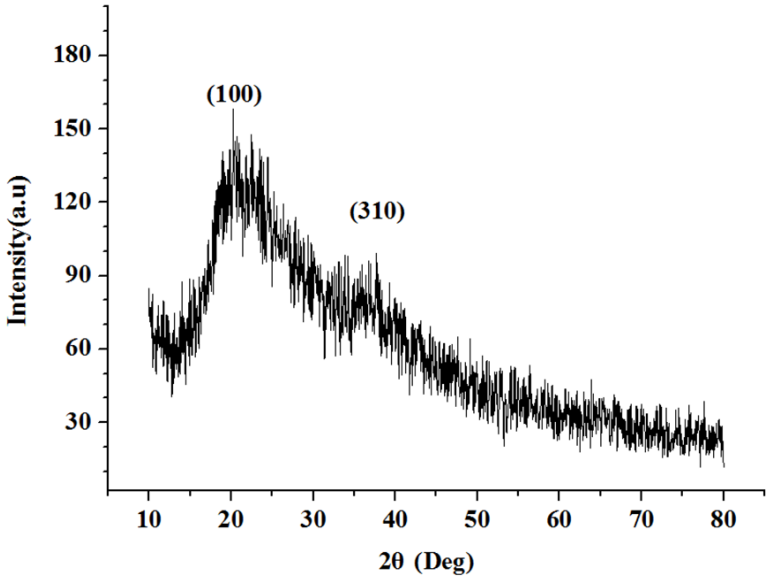


**Figure S1.** XRD pattern of HSA-$MnO_2$ NPs.

The X-ray diffraction (XRD) profile of the HSA-$MnO_2$ NPs exhibited a distinct peak at $2\theta = 21.06°$, which was in line with characteristic peaks of $MnO_2$ (Figure S1).

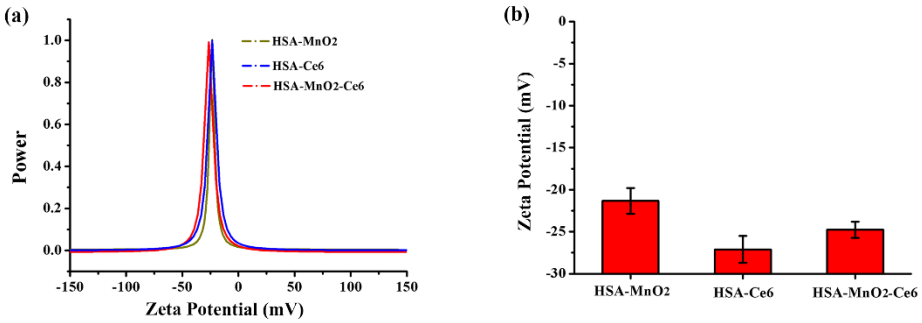


**Figure S2.** Zeta potential of HSA-$MnO_2$ NPs, HSA-Ce6 NPs, and HSA-$MnO_2$-Ce6 NPs. Error bars indicate standard deviations of three independent measurements.

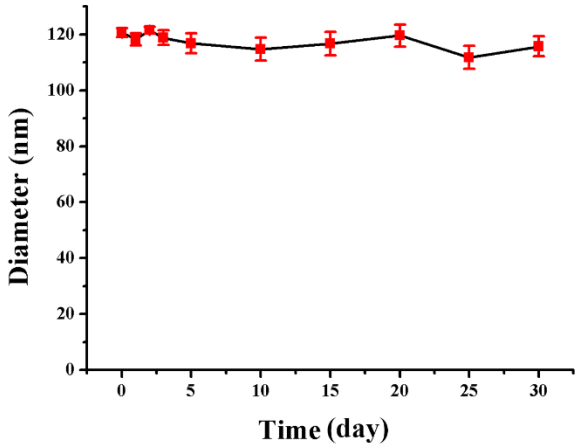


**Figure S3.** Colloidal stability of HSA-$MnO_2$-Ce6 NPs measured by time-dependent DLS. Error bars indicate standard deviations of three independent measurements.

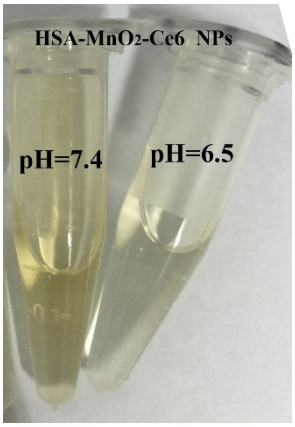


**Figure S4.** Images of HSA-$MnO_2$-Ce6 NPs incubated in pH 7.4 or pH 6.5 buffer for 12 h.

The visual images of HSA-$MnO_2$-Ce6 NPs incubated for 12 h in different pH buffers are shown in Figure S4. The color of the NP solution disappeared at pH 6.5, which suggested the complete decomposition of $MnO_2$ into $Mn^{2+}$.

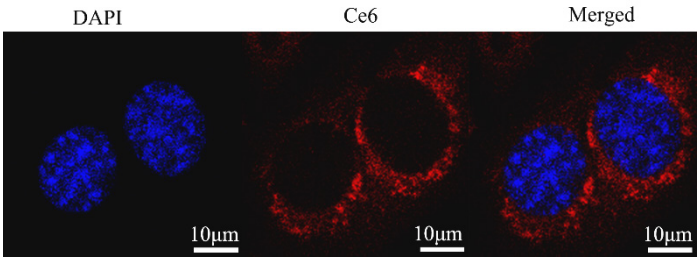


**Figure S5.** Confocal image of individual cells after incubation with HSA-$MnO_2$-Ce6 NPs.

The amplified confocal images shown in Figure S5 revealed the single cell uptake of HSA-$MnO_2$-Ce6 NPs.

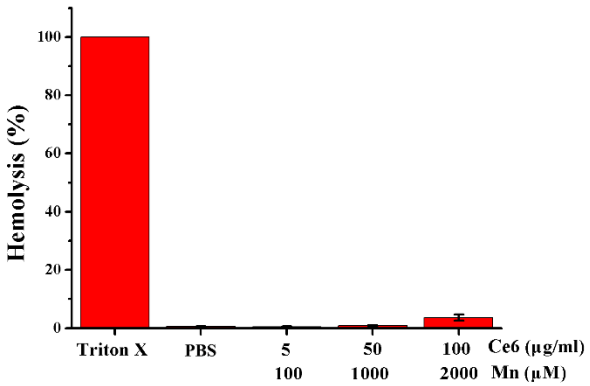


**Figure S6.** Hemolytic effect of HSA-$MnO_2$-Ce6 NPs. Error bars indicate standard deviations of three independent measurements.

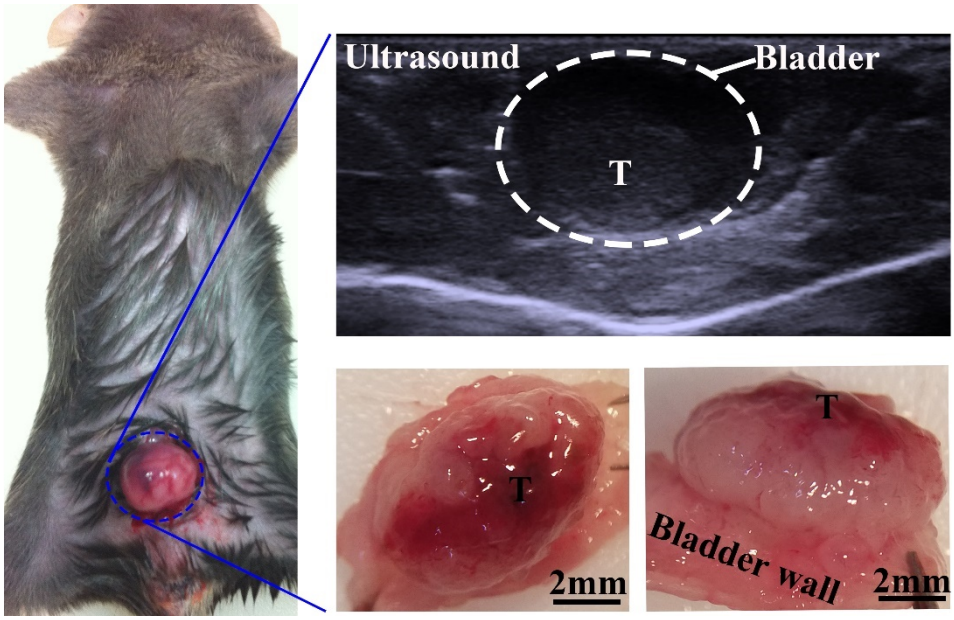


**Figure S7.** Orthotopic bladder cancer model in C57BL/6 mice. T, tumor.

We established the orthotopic bladder cancer model in C57BL/6 mice according to our previous report.[1] Photographs of orthotopic bladder cancer are in Figure S7. Ultrasonography showed a low echogenic tumor area in bladder. Photos of autopsies also showed an obvious solid lesion in bladder, which indicated the successful establishment of orthotopic bladder cancer.

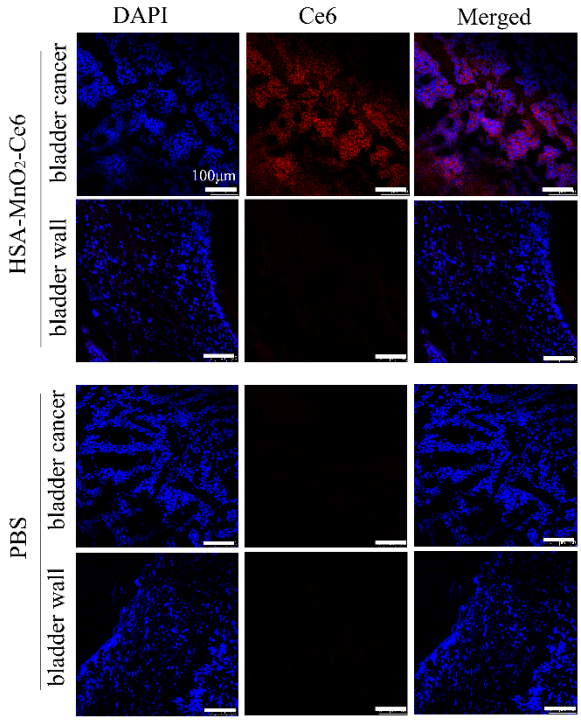


**Figure S8.** Confocal images of bladder cancer slices. The red fluorescent intensity of NPs was high in bladder cancer tissues but no fluorescence was observed in bladder wall.

As the confocal images showed, the fluorescent intensity of NPs was high in bladder cancer tissues, but no fluorescence of NPs was observed in bladder wall (Figure S8). Therefore, it further confirmed that the NPs were accumulated in the tumor region instead of in normal bladder tissues.

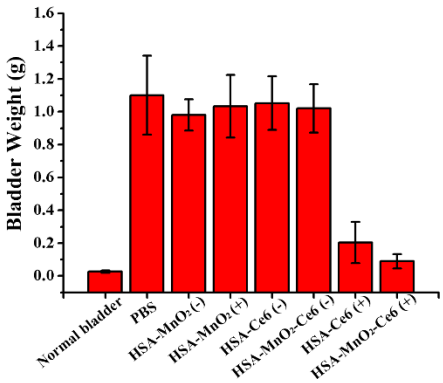


**Figure S9.** Bladder weight of mice after treatment. Error bars indicate standard deviations of four independent measurements.

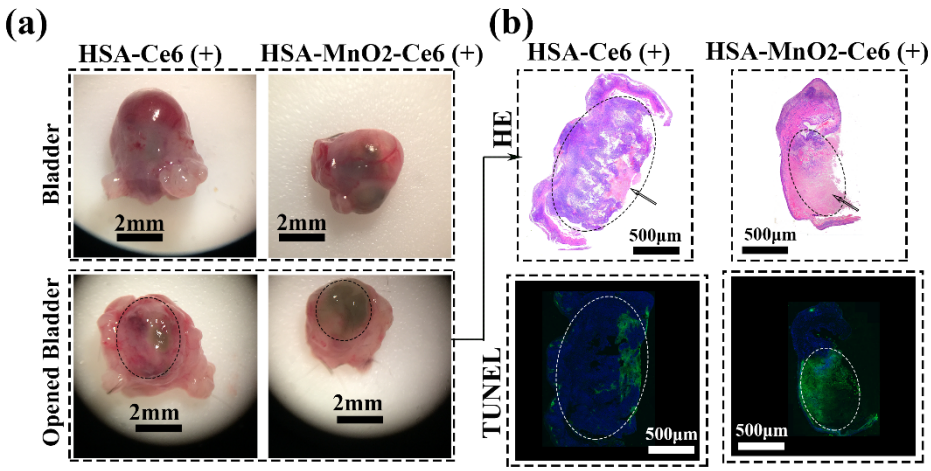


**Figure S10.** (a) Comparison of HSA-$MnO_2$-Ce6 and HSA-Ce6 NP therapeutic efficacy. Black dotted circles indicate residual bladder cancer areas. (b) HE sections (black dotted circles indicate residual bladder cancer areas) and TUNEL sections (white dotted circles indicate residual bladder cancer areas) for (a). Black arrow in HE sections indicates necrosis area and green areas in TUNEL sections represent cell apoptosis.

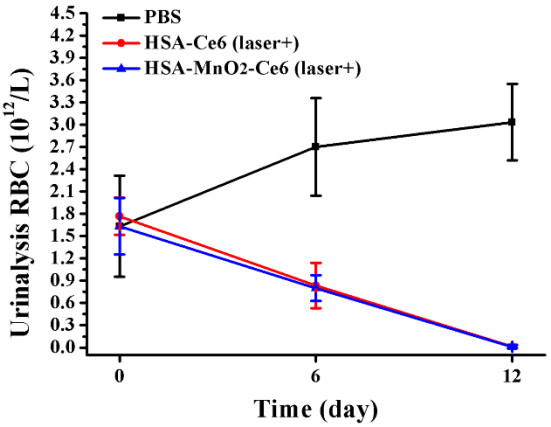


**Figure S11.** Urinary red blood cell count to evaluate the photodynamic effect on hematuria. Error bars indicate standard deviations of four independent measurements.

Hematuria is the typical symptom of bladder cancer, which is due to the superficial tumor diabrosis and hemorrhage in bladder lumen. We tested urinary red blood cell counts to evaluate the photodynamic effect on hematuria (Figure S11). Severe hematuria in mice without PDT was observed. Hematuria was significantly alleviated on day 6 and was almost disappeared on day 12 after PDT. These results further confirmed that the bladder cancers were ablated by photodynamic effect.

## References

1. Lin, T. S.; Yuan, A.; Zhao, X. Z.; Lian, H. B.; Zhuang, J. L.; Chen, W.; Zhang, Q.; Liu, G. X.; Zhang, S. W.; Chen, W.; Cao, W. M.; Zhang, C. W.; Wu, J. H.; Hu, Y. Q.; Guo, H. Q. Self-assembled tumor-targeting hyaluronic acid nanoparticles for photothermal ablation in orthotopic bladder cancer. *Acta Biomater.* **2017,** *53*, 427-438.